

This is the author-created version of the following work:

Chinnappan, Raja, Rahamn, Anas Abdel, AlZabn, Razan, Kamath, Sandip, Lopata, Andreas L., Abu-Salah, Khalid M., and Zourob, Mohammed (2020)
Aptameric biosensor for the sensitive detection of major shrimp allergen, tropomyosin. Food Chemistry, 314 .

Access to this file is available from:

<https://researchonline.jcu.edu.au/63527/>

© 2019 Elsevier Ltd. All rights reserved.

Please refer to the original source for the final version of this work:

<https://doi.org/10.1016/j.foodchem.2019.126133>

2 **Aptameric biosensor for the sensitive detection of major shrimp**
3 **allergen, tropomyosin**

4
5 Raja Chinnappan^{#a}, Anas Abdel Rahamn^{#b,c,d}, Razan AlZabn^a Sandip Kamath^{e,f}, Andreas L.
6 Lopata^{e,f}, Khalid M. Abu-Salah^g, Mohammed Zourob^{a,b*}

7

8 ^a Department of Chemistry, Alfaisal University, Al Zahrawi Street, Al Maather, Al
9 Takhassusi Road, Riyadh 11533, Saudi Arabia

10 ^b Department of Genetics, King Faisal Specialist Hospital, and Research Center, Zahrawi
11 Street, Al Maather, Riyadh 11211, Saudi Arabia.

12 ^c College of Medicine, Alfaisal University, Al Zahrawi Street, Al Maather, Al Takhassusi
13 Road, Riyadh 11533, Saudi Arabia

14 ^d Department of Chemistry, Memorial University of Newfoundland, St. John's, NL, A1B
15 3X7, Canada

16 ^e College of Public Health, Medical, and Veterinary Sciences, Department of Molecular &
17 Cell Biology, James Cook University, Townsville, QLD, Australia.

18 ^f Molecular Allergy Research Laboratory, Australian Institute of Tropical Health and
19 Medicine, James Cook University, Townsville, QLD, Australia.

20 ^g Department of Nanomedicine, King Abdullah International Medical Research Center/King
21 Saud Bin Abdulaziz University for Health Sciences, King Abdulaziz Medical City, Riyadh
22 11481, Saudi Arabia.

23

24 # Equal contribution

25 ***Corresponding author:**

26 **E-mail: mzourob@alfaisal.edu**

27

Abstract

The development of a sensitive and rapid detection approach for allergens in various food matrices is essential to assist patients in managing their allergies. The most common methods used for allergen detection are based on immunoassays, PCR and mass spectrometry. However, all of them are very complex and time-consuming. Herein, an aptamer biosensor for the detection of the major shrimp allergen tropomyosin (TM) was developed. Graphene oxide (GO) was used as a platform for screening of the minimal-length aptamer sequence required for high-affinity target binding. A fluorescein dye labeled GO quenches the truncated aptamer by π -stacking interactions. After the addition of TM, the fluorescence was restored due to the competitive binding of the aptamer to GO. One of the truncated aptamers was found to bind to TM with four-fold higher affinity (30 nM) compared to the full-length aptamer (124 nM), with a limit of detection (LOD) of 2 nM. The aptamer-based sensor demonstrates the sensitive, selective, and specific detection of TM in 30 min. The performance of the sensor was confirmed using TM spiked chicken soup, resulting in a high percentage recovery ($\sim 97 \pm 10\%$). The association of GO and labelled aptamer sensor platform has shown the rapid detection of TM in food, which is compared to other methods very sensitive, specific and performs in high throughput application.

46

Keywords: Aptasensor, analytical assay, graphene oxide, tropomyosin, fluorescence assay, shellfish-allergens, allergen detection, food safety.

49

50 1. Introduction

51 The prevalence of shellfish allergy in the increasing worldwide affecting up to 5% of
52 consumers. Shellfish are divided into two groups, the crustaceans and mollusks, including
53 commonly consumed species including shrimps, crabs, lobsters and gastropods, cephalopods
54 and bivalves respectively. Shrimp is the predominant species causing over 80% of reactions
55 to shellfish that result in severe clinical outcomes. Tropomyosin is one of the major allergic
56 proteins found in shrimp and highly stable even at high temperatures(Lopata, Kleine-Tebbe,
57 & Kamath, 2016).

58 The current allergen detection methods are mainly based on enzyme-linked immunosorbent
59 assay (ELISA), DNA detection, microarray(Lupinek, Wollmann, Baar, Banerjee,
60 Breiteneder, Broecker, et al., 2014) and qualitative/semi-quantitative lateral flow assays
61 (Sharma, Khuda, Parker, Eischeid, & Pereira, 2016). ELISA is the most commonly used
62 method for the TM detection and quantification (Fuller, Goodwin, & Morris, 2006; Kamath,
63 Abdel Rahman, Komoda, & Lopata, 2013; Kamath, Thomassen, Saptarshi, Nguyen, Aasmoe,
64 Bang, et al., 2014; Seiki, Oda, Yoshioka, Sakai, Urisu, Akiyama, et al., 2007; Werner, Fæste,
65 & Egaas, 2007; Y. Zhang, Wu, Wei, Zhang, & Mo, 2017). The homology in amino acid (AA)
66 sequence of TM between crustaceans and mollusks ranges from 55-65% (Ruethers, Taki,
67 Johnston, Nugraha, Le, Kalic, et al., 2018). However, among the crustacean group the
68 sequence homology ranges from 88-100%, with the highest homology between different
69 shrimp species with >95% homology. Due to this various levels of aa sequence homology,
70 the resulting potential immunological cross-reactivities pose a challenge for antibody based
71 ELISAs to distinguish between crustaceans and mollusks TM (Fernandes, Costa, Oliveira, &
72 Mafra, 2015; Kamath, Abdel Rahman, Komoda, & Lopata, 2013).

73

74 Mass spectrometry has been applied for the detection and quantification of food allergens to
75 overcome the drawbacks of immunological-based techniques. Allergens from several
76 shellfish species prawns (Khanaruksombat, Srisomsap, Chokchaichamnankit, Punyarit, &
77 Phiriyangkul, 2014; Koeberl, Clarke, & Lopata, 2014; Koeberl, Kamath, Saptarshi, Smout,
78 Rolland, O'Hehir, et al., 2014), crab (Koeberl, Clarke, & Lopata, 2014) and cephalopod
79 (Shen, Cao, Cai, Ruan, Mao, Su, et al., 2012) have been analyzed utilizing different mass
80 spectrometric techniques. Abdel Rahman et. al. have identified signature peptides for Black
81 Tiger prawn, Northern prawn, and Snow crab, and then utilized these peptides for developing
82 liquid chromatography (LC) coupled with multiple reaction monitoring (MRM) mass
83 spectrometer methods for species-specific allergens quantification (Abdel Rahman, Kamath,
84 Gagné, Lopata, & Helleur, 2013; Rahman, Gagné, & Helleur, 2012; Rahman, Kamath,
85 Lopata, & Helleur, 2010; Rahman, Kamath, Lopata, Robinson, & Helleur, 2011; Rahman,
86 Lopata, Randell, & Helleur, 2010). However, mass spectrometric analysis, immunoassays
87 and PCR techniques are time-consuming and rely on skilful operators and expensive
88 instruments. Therefore, rapid and low-cost biosensors, which can be used as point-of-care for
89 the detection of TM is highly needed to help allergic patients with their preventive measures.
90 Several biosensor-based techniques have been developed for the sensitive detection of TM
91 from food sources. A recent report on the ultrasensitive detection of TM using aptamer-based
92 photoelectrochemical methods and utilizing graphitic carbon nitride-TiO₂ nanocomposite
93 (Amouzadeh Tabrizi, Shamsipur, Saber, Sarkar, & Ebrahimi, 2017) overcomes the
94 disadvantages of the antibody-based allergen detection.

95

96 Aptamers consist of single-stranded DNA, RNA or peptides that bind to the target molecule
97 with high affinity (K_{ds} in nanomolar to the picomolar range) and specificity. Aptamers are
98 selected for a vast variety of targets including metal ions, pathogens, small organic

99 molecules, and viruses. Systematic Evolution of Ligands by Exponential Enrichment
100 (SELEX) method is used to determine the right aptamer for the targeted analyte from a library
101 of chemically synthesised random sequences (containing approximately 10^{15}
102 oligonucleotides). Biosensors developed for the detection of targets using the right aptamer as
103 a recognition receptor. Aptamer-based biosensors have shown multiple advantages over
104 antibodies such as in vitro selection, high stability, low cost of chemical synthesis and post
105 modifications (Lapa, Chudinov, & Timofeev, 2016). The ideal aptamer consists of 40-100
106 nucleotides. Under suitable conditions, the aptamer can form secondary and tertiary
107 structured binding pockets which can capture the target to form strong aptamer-target
108 complexes.

109 Aptamer-based sensors undergo a significant conformational change upon target recognition,
110 which leads to a change in the transducer signals. Though the aptamers are specific to their
111 targets, post SELEX optimizations such as eliminating non-essential nucleotides will improve
112 the affinity and the specificity considerably. A significant improvement in the binding
113 affinity of anti-Salmonella enteritidis and anti-progesterone truncated aptamer have been
114 achieved by removing the non-essential nucleotides from the parental aptamer (H.
115 Alhadrami, R. Chinnappan, S. Eissa, A. A. Rahamn, & M. Zourob, 2017; Chinnappan,
116 AlAmer, Eissa, Rahamn, Salah, & Zourob, 2018). Zhang et al. have reported 40 nucleotide
117 ssDNA aptamer obtained from the dot-blotting SELEX (Y. Zhang, Wu, Wei, Zhang, & Mo,
118 2017). As GO is an efficient energy acceptor (Ding, Cargill, Das, Medintz, & Claussen,
119 2015; Yang, Asiri, Tang, Du, & Lin, 2013), we used GO as a sensing platform for probing
120 the high-affinity binding sequences from wild-type aptamer of anti-TM.

121 This study aims to develop an aptamer-based biosensor for the sensitive detection of the
122 major shellfish allergen TM, using high-affinity fluorescein truncated ssDNA aptamers and
123 GO as a sensing platform. Anti-TM aptamers has been reported recently, however the cross-

124 reactivity of the sensor was neither examined or validated with close relevant proteins or real
125 samples(Y. Zhang, Wu, Wei, Zhang, & Mo, 2017). In this study we probed for high-affinity
126 binding sequences from the parental aptamer to develop an efficient aptasensor. Cross-
127 reactivity studies with different TM proteins derived from Shrimp, Oyster and anisakis were
128 evaluated and further validation studies of the sensor were conducted to analyze and
129 estimated the amount of spiked protein in the chicken noodle soup. We demonstrate here
130 that the new developed sensor has high sensitivity for TM from shrimp and can be used for
131 the analysis of food for contamination.

132 2. Experimental

133 134 2.1 Materials and Methods

135 Natural tropomyosin from black tiger prawn (*Penaeus monodon*) and Oyster (*Crassostrea*
136 *gigas*) were purified using ammonium sulphate precipitation method as described previously
137 (Nugraha, Kamath, Johnston, Zenger, Rolland, O'Hehir, et al., 2018). Recombinant prawn
138 (*Penaeus monodon*) tropomyosin (rPen m 1) and recombinant anisakis (*Anisakis simplex*)
139 tropomyosin (rAnis3) was expressed and purified as described previously (Asnoussi, Aibinu,
140 Gasser, Lopata, & Smooker, 2017; Koeberl, et al., 2014). N-Hydroxysuccinimide (NHS)
141 activated sepharose-4B was purchased from GE healthcare (Milwaukee, WI, USA). Phosphate
142 buffered saline (PBS) tablets, Tris base, sodium chloride, sodium acetate, sodium
143 bicarbonate, sodium azide hydrochloric acid, magnesium chloride streptavidin and bovine
144 serum albumin (BSA) were obtained from Sigma-Aldrich (St Louis, MO, USA). Graphene
145 oxide (GO) dispersion was supplied by Dropsens Inc. (Asturias, Spain). HPLC purified
146 labeled, and unlabeled oligonucleotides were provided by Metabion International (Planegg,
147 Germany). The DNA oligonucleotides were dissolved in ultrapure Milli-Q water to make the
148 stock solutions and stored at -20°C until further use. The DNA solutions used in the

149 experiments were diluted with binding buffer. The fluorescein-labeled oligonucleotides were
150 protected from light while performing the experiments.

151 **2.2 Fluorescence Measurements**

152 All the fluorescence measurements for the fluorescein-labeled aptamers, the complementary
153 oligonucleotides, and the beacon, were performed using Nanodrop ND3300
154 fluorospectrometer (Thermo Scientific, Canada). The samples were excited under blue light
155 (470 ± 10 nm), and the emission monitored at 515 nm. All the measurements were recorded in
156 the binding buffer (50mM Tris, 150mM NaCl, 2mM $MgCl_2$ pH, 7.4) at room temperature in
157 triplicate unless otherwise mentioned. The fluorescence spectra presented were the average of
158 three measurements.

159 **2.3 Preparation of Tropomyosin conjugated sepharose beads**

160 Tropomyosin was conjugated with NHS activated sepharose-4B beads according to the
161 protocol as reported previously (H. A. Alhadrami, R. Chinnappan, S. Eissa, A. A. Rahamn, &
162 M. Zourob, 2017). Briefly, sepharose-4B beads were washed with 10-15 volumes of 1mM
163 HCl followed by coupling buffer (50 mM carbonate buffer, pH= 9.2). One mg of TM was
164 added to the slurry of washed sepharose-4B beads and mixed for three hours in 50 mM
165 carbonate buffer (pH= 9.2) at room temperature. The TM conjugated beads were washed with
166 carbonate buffer to remove the unreacted TM. The unreacted active sites in the beads were
167 quenched by treating with 50 mM tris (pH=8) for 1 hour, and then washed with 50 mM Tris,
168 0.5M NaCl pH=8 and 50 mM sodium acetate, 0.5 M NaCl pH = 4.5 alternatively for 6 times.
169 The washed beads were stored in 10 mM Tris pH = 7.5 and 0.05% sodium azide at 4°C until
170 further use.

171 **2.4 Design of truncated aptamer**

172 As it was assumed the constant primer binding sites of the aptamers are not involved in the
173 formation of aptamer-target complexes, we considered the random sequences of flanked

174 regions of the aptamers' library for our design. Two different variants of the truncated
175 aptamer have been designed from the secondary structure of the aptamer obtained by m-fold
176 software (at 150 mM NaCl, 2mM Mgcl₂ at 25°C). The original parental anti-tropomyosin
177 aptamer sequence was obtained from a previous report (Y. Zhang, Wu, Wei, Zhang, & Mo,
178 2017). The first aptamer consists of 14 nucleotides (TMT1) and the second variant consists of
179 26 nucleotides (TMT2) as shown in Fig.1. Both aptamers were labeled with fluorescein at the
180 5'end and were used for the determination of the dissociation constants and the GO-based
181 biosensors developments.

182 **2.5 Determination of the binding affinity of the truncated aptamer**

183 To find the high affinity truncated aptamer with TM, each aptamer sequence was labeled with
184 fluorescein. The fluorescein-labeled truncated aptamers were heated to 90°C for 5 minutes,
185 4°C for 10 minutes and room temperature for 10 minutes. Variable concentrations of
186 fluorescein-labeled aptamers (0-250 nM) were incubated with tropomyosin conjugated beads
187 for one hour. The unbound aptamers were removed by washing with binding buffer. The
188 bound DNA was eluted with the elution buffer (7 M urea in 50 mM tris+150 mM +NaCl mM
189 +2 MgCl₂). The fluorescence intensities of the eluted DNA from beads were plotted against
190 the concentration of input DNA aptamer. The dissociation constant (K_d) of each aptamers
191 were calculated from the saturation curve by non-linear regression fitting using Prism five
192 software.

193 **2.6 Optimization of Graphene oxide/aptamer ratio and detection**

194 Based on the fluorescence intensity, the concentration of the labeled truncated aptamers has
195 been optimized and used for further experiments. The GO to aptamer ratio were optimized by
196 titrating the 25 nM aptamer with increasing concentration of GO in the rage of 0-50 µg/ml in
197 binding buffer. After the addition of GO to the aptamer solution, the mixture was incubated at
198 room temperature for 30-35 minutes to achieve maximum adsorption of aptamer on the GO

199 surface. A dynamic range of (0 to 50 $\mu\text{g/ml}$) of TM in binding buffer was incubated with the
200 mixture of GO-aptamer (15 $\mu\text{g/ml}$ - 25nM) for 30-35 minutes. The fluorescence of each
201 sample was measured with the excitation and emission wavelengths of 470 ± 10 nm and 515
202 nm respectively. The calibration curve was obtained by plotting the fluorescence intensity
203 changes against the concentration of TM used. The selectivity and cross-reactivity of the
204 biosensor platform were tested with BSA, streptavidin and the analog of recombinant
205 tropomyosin proteins such as prawn (*Penaeus monodon*) recombinant tropomyosin, anisakis
206 (*Anisakis simplex*) recombinant TM and oyster (*Crassostrea gigas*) native TM.

207 **3. Results and Discussion**

208 Aptamers with high affinity towards the target analyte are an essential criterion. Aptamers
209 obtained by conventional SELEX are selected from libraries with 40-60 flanking sequences.
210 Elimination of non-essential nucleotides from unique binding pocket allows for better
211 interaction with target molecules. The constant primer sequences region of the aptamer shows
212 minimal involvement in target binding (Cowperthwaite & Ellington, 2008; Jayasena, 1999).
213 However, the truncation of anti-acetylcholinesterase aptamer showed a significant
214 contribution of the constant primer regions towards binding to the target (Le, Chumphukam,
215 & Cass, 2014). The secondary structure of ssDNA aptamer such as the stem-loop, G-
216 quadruplex, bulges, and pseudoknots in association with the tertiary structures are essential
217 for target binding (Hasegawa, Savory, Abe, & Ikebukuro, 2016; Kaur & Yung, 2012). The
218 recognition of conformational changes in the aptamer upon target binding is critical in
219 biosensor applications. The binding sites of the aptamer may be predicted from the secondary
220 structure followed by the sequence truncation, which could improve the affinity and
221 fabrication of cost-effective biosensor platform (Zhou, Battig, & Wang, 2010).

222 **3.1 Determination of high-affinity aptamer sequence region**

223 Zhang et. al. selected ssDNA aptamer for shrimp TM, by dot-spotting SELEX method, where
224 the dissociation constant of the high-affinity aptamer A5 and A15 are reported as 109 and
225 127 nM, respectively (Y. Zhang, Wu, Wei, Zhang, & Mo, 2017). Based on the above
226 considerations and m-fold secondary structure prediction, the parental aptamer A15 was
227 truncated into two regions as shown in **Fig. 1**. The secondary structure of anti-TM aptamer
228 consists of 40 nucleotides length excluding the primer binding sites (**Fig.1**). Truncation of the
229 position at site 15 from the 5' end leads to a couple of different short aptamers, where the first
230 one (14 nucleotides) has a stem-loop structure (TMT1) (**Fig.1A**). The second variant (25
231 nucleotides) has stem-loop and a bulge in the middle of the stem (TMT2) (**Fig.1B**). In order
232 to compare the reported dissociation constant (K_d) of the parental aptamer, the parent aptamer
233 was fluorescently labeled and incubated with TM conjugated sepharose beads. The K_d was
234 calculated by fitting the saturation curve obtained from the fluorescence intensity against the
235 concentration of the corresponding aptamer (**Fig.2A**). The obtained K_d value is 115 ± 20 nM
236 which is comparable with the previously reported 124 nM obtained from the enzyme-linked
237 aptamer assay (ELAA) (Y. Zhang, Wu, Wei, Zhang, & Mo, 2017). Similarly, we obtained the
238 plot for the two truncated variants as shown in **Fig.2B**. Saturated fluorescence intensity was
239 not attained as the concentration of TMT1 aptamer increased due to the lack of binding
240 between the TMT1 and TM. Since a very short aptamer (8 nucleotides long) has been
241 reported for a sensitive colorimetric detection approach of tetracycline (Kwon, Raston, & Gu,
242 2014), we assumed that 14 nucleotides TMT1 aptamer could bind to TM. In other words, this
243 region of the parental aptamer is not essential for the formation of the aptamer-target
244 complex. The dissociation constant, 30 ± 15 nM, of TMT2 obtained from the saturation curve
245 reveals that this region of the aptamer is involved in TM binding. Approximately four-fold
246 enhancement in the binding affinity of TMT2 implies that the truncated aptamer may form a
247 unique secondary structure in the presence of $MgCl_2$, and NaCl at the given pH condition,

248 which ideally allows capturing TM with high affinity. This indicates the major role of TMT2
249 in the direct binding process and form an aptamer-TM complex. The same aptamer has been
250 used for the development of GO-based fluorescence biosensor for the detection of TM.

251 **3.2 Graphene oxide as a biosensor platform**

252 Graphene oxide (GO) is a two dimensional (2D) aromatic structured material, which consists
253 of multiple layers of graphene sheets. GO is an ideal candidate for the surface adsorption of
254 many biomolecules such as proteins, peptide, DNA, RNA, bacteria and small organic
255 molecules (Huan Zhang, Zhang, Aldalbahi, Zuo, Fan, & Mi, 2017). GO is considered as a
256 much better quencher compared to the usual quencher molecules(Gao, Li, Li, Yan, Zhou,
257 Chen, et al., 2015). GO quenches the fluorescence of the molecules by fluorescence
258 resonance energy transfer (FRET) mechanism. It has been reported that GO interact with
259 ssDNA strongly by non-covalent interactions such as π - π stacking and hydrophobic
260 interactions and quenches the fluorescence of labeled DNA completely (Chinnappan,
261 AlAmer, Eissa, Rahamn, Salah, & Zourob, 2018; Stobiecka, Dworakowska, Jakiela,
262 Lukasiak, Chalupa, & Zembrzycki, 2016). As TMT2 has a higher affinity constant, we used
263 fluorescein labeled truncated aptamer (TMT2) and GO-based fluorescence switching assay
264 for TM detection. This method consists of two steps; GO quenches the fluorescence of the
265 Flu-TMT2 by FRET, in the second step, when the TM was introduced, Flu-TMT2 detach
266 from the GO surface and form Flu-TMT2-TM complex. The amount of TM-aptamer complex
267 suspended in the solution was correlated with the TM concentration through the fluorescence
268 intensity. Therefore, the amount of TM was reflected by the fluorescence intensity as
269 represented in Scheme-1.

270 **3.3 Optimization of GO/Aptamer ratio by fluorescence quenching**

271 The concentration of the Flu-TMT2 aptamer used in this experiment was optimized to be 25
272 nM, where the fluorescence intensity gave a significant signal to noise ratio (s/n). To get the

273 minimum GO concentration required for better quenching performance of Flu-TMT2
274 fluorescence, a fixed amount of aptamer (25 nM) was titrated with a wide range of GO
275 concentration from 0 to 50 $\mu\text{g}/\text{ml}$. In the absence of GO, the Flu-aptamer showed a strong
276 fluorescence intensity as shown in **Fig.3**. Upon addition of increasing concentration of GO,
277 the fluorescence intensity started to decrease and completely disappeared at 35 $\mu\text{g}/\text{ml}$ of GO
278 (**Fig 3A, Insert: a - k**). There was no further change in fluorescence intensity with increasing
279 GO concentration which indicates that most of aptamer molecules were stacked on the GO
280 surface and become completely off state. The plot of fluorescence intensity against the
281 concentration of GO shows that 88% quenching at the GO concentration of 15 $\mu\text{g}/\text{ml}$ was
282 attained (**Fig.3B**). The ratio of 25 nM of TMT2 for 15 $\mu\text{g}/\text{ml}$ of GO has been used as the
283 optimal off state for the rest of the experiments.

284 **3.4 Graphene oxide based aptasensor for Tropomyosin detection**

285 The graphene oxide-based biosensor platform for the detection of TM was established as
286 before (GO/aptamer ratio). As discussed, the full-length aptamer was used for the detection
287 of tropomyosin using GO and DNA intercalating fluorescent dye as a probe. Herein the
288 fluorescent truncated aptamer was used as a recognizing element. As shown in **Fig.4**, the
289 fluorescence of GO-aptamer increases linearly by addition of increasing concentration of TM
290 from 0 to 50 $\mu\text{g}/\text{ml}$. Tropomyosin triggered the fluorescence signal by detaching the aptamer
291 from the GO surface to the solution state. The fluorescence intensity of the released aptamer
292 was plotted against the concentration of TM to generate a calibration curve to determine the
293 detection limit (LOD), and linearity as shown in **Fig.4B**. The LOD was calculated as 3.3
294 SD/s , where SD is standard deviation of the signal of blank samples and s is the slope of the
295 linear calibration curve. The calculated LOD suggested that the TMT2 aptamer is more
296 sensitive compared to the original aptamer. TMT2 has the LOD of 2.5 nM, which is two-fold
297 higher in sensitivity than the previously reported LOD for the full length aptamer sequence

298 (Y. Zhang, Wu, Wei, Zhang, & Mo, 2017). The enhancement in the LOD is presumably due
299 to the elimination of the non-essential nucleotides from the full-length aptamer which may
300 not be involved in the formation of the binding pocket essential for capturing the target.
301 Moreover, the presence of these non-binding nucleotides enhances the secondary and tertiary
302 structure of the aptamer, which reduces the chance of binding to TM. The LOD of this novel
303 GO-based aptasensor is comparable with the previously reported results generated by
304 expensive and sophisticated instruments. For example, the TM extracted from whole shrimp
305 was estimated by ELISA method with LOD of 1 ppm (1-2 $\mu\text{g/g}$) (Fuller, Goodwin, & Morris,
306 2006). A sandwich ELISA was reported for the detection of kuruma prawn TM using CE7B2
307 monoclonal antibody with the sensitivity of 90 pg/ml (Hong Zhang, Lu, Ushio, & Shiomi,
308 2014). Werner et al. reported the detection of TM from various food matrices, had an LOD
309 of 1.6 $\mu\text{g/g}$ which is comparable to our method (Werner, Fæste, & Egaas, 2007). Tabrizi et al
310 developed a photoelectrochemical method for the detection of TM using graphitic carbon
311 nitride and titanium dioxide as photoactive materials with LOD of 0.23 ng/g (Amouzadeh
312 Tabrizi, Shamsipur, Saber, Sarkar, & Ebrahimi, 2017; Werner, Fæste, & Egaas, 2007). This is
313 a relatively more sensitive method compared to our method. However, the fabrication of the
314 photoelectrochemical sensor is a multistep process that involves the utilization of several
315 sophisticated instruments such as SEM, TEM, AFM, X-ray, FTIR etc. Real time PCR (RT-
316 qPCR) based assay was reported for the detection of shrimp TM allergen using shrimp
317 tropomyosin gene. Though the detection limit is 3.2 pg , the method is associated with
318 sophisticated thermocyclers for RT-qPCR amplification (Kim, Kim, Kim, Suh, & Kim,
319 2019). In addition, it is a time-consuming process and requires well trained technicians
320 compared to GO-based fluorometric aptasensor that has been developed in this study.

321

322 3.5 Selective binding of aptamer

323 The binding selectivity between TM and TMT2 was determined by examining the sensor
324 with closely related as well as not related proteins. The cross reactivity of the sensor was
325 evaluated with the allergen TM purified from tiger prawn (*penaeus monodon*), Aniskis
326 (*Aniskis simplex*), and oyster (*Crassostrea gigas*) muscle. In addition, the cross reactivity was
327 examined with other non-related proteins such as streptavidin and BSA as shown in **Fig.5**.
328 TMT2 aptamer cross reacted with recombinant tropomyosin from prawn and Oyster with
329 80% and 75%, respectively, while 50% cross reactivity was observed with Aniskis
330 recombinant TM. Other proteins such as streptavidin and BSA demonstrated less than 25%
331 cross reactivity with TMT2 aptamer. The amino acid sequences of crustacean TM has a more
332 conservative region in different species, which increases the cross reactivity with the
333 truncated aptamer. In this study, tropomyosin from prawn (crustacean), oyster (mollusc) and
334 anisakis (seafood parasitic nematode) were tested. Oyster and anisakis TMs have 62% and
335 72% amino acid sequence identity respectively with TM from shrimp. As TMT2 can
336 recognition TM recombinants, it can also be used as a recognising element for detection of
337 TM in various seafood species. Eventually, the GO-TMT2 fluorescence biosensor will be an
338 ideal platform for the detection of recombinant and purified naturally occurring major
339 seafood allergen.

340 **3.6 Validation of GO-aptamer sensor with spiked samples**

341 The developed sensor has been validated with chicken noodle soup obtained from the local
342 market after spiking with shrimp TM. The original soup was diluted 10 times and spiked with
343 TM at a final concentration of 2, 5 and 10 µg/ml. The TM extraction recovery of the spiked
344 samples are summarised in Table-S1 (in the supporting information). The recovered amount
345 of TM that has been measured with the new developed sensor was concordant (close to 100%
346 recovery) with the spiked amount, supporting the reliability of the sensor for detecting TM in
347 food preparations.

348 4. Conclusions

349 In summary, a high affinity binding pocket of the aptamer was probed in this study, which
350 can bind to invertebrate TM. The non-essential part of the sequence of the suggested aptamer
351 was truncated for better binding to the target molecule and the affinity increased four-folds
352 after this truncation. The affinity of the fluorescent aptamer was high enough to be used for
353 the development of the GO-based fluorescence assay. The sensitivity of the method increased
354 more than two folds with LOD of 2.5 nM compared to the full-length aptamer sequence. This
355 method was highly selective to shrimp TM. Nevertheless, a significant cross-reactivity was
356 observed to TM of other invertebrate species due to the overall high similarity in their protein
357 amino acid sequences. Finally, the detection and high recovery of TM in chicken soup spiked
358 with TM, support the potential of this sensor to be applied in food analysis. Though, the
359 inhomogeneous consistency of food products is the major challenge for implementation of
360 this method, diluting the sample can eliminate this problem. This method could detect TM of
361 not only shellfish, but can also be used for the detection of different TM allergens from
362 various food sources using specific aptamers. Moreover, the high sensitivity and simplicity
363 will allow multiple target detection using different fluorophore labelled aptamers.

364

365

366

367 **Figure Captions**

368

369 **Scheme.1:** Schematic diagram represents fluorescence switching in graphene oxide based
370 fluorescence assay for Tropomyosin

371

372 **Fig.1.** (A) Secondary structure of full-length TM aptamer. (B) Secondary structure 14

373 nucleotide truncated aptamer (TMT1). (C) Secondary structure of 25 nucleotide truncated

374 aptamer (TMT2).

375

376 **Fig. 2.** Saturation binding affinity curve obtained from the titration of TM with TM-

377 conjugated sepharose beads. (A) Full-length aptamer, (B) Truncated aptamers (TMT1 and

378 TMT2). The error bars represent standard deviation obtained from three different

379 measurements. The fluorescence spectra were recorded by exciting at 470 ± 10 nm and the

380 emission intensity 515 nm used for the plots. The error bars represent the standard deviation

381 of three different measurements.

382 **Fig.3.** (A) Fluorescence intensity of TMT2 (25nM) with increasing concentration of graphene

383 oxide (GO) a: 0, b: 5, c: 10, d:15, e: 20, f: 25, g: 30, h: 35, I: 40, j: 45, k: 50 $\mu\text{g/ml}$. (B) Plot

384 GO concentration vs Fluorescence intensity of TMT2 at 515 nm (λ -max). The fluorescence

385 spectra were recorded by exciting at 470 ± 10 nm and the emission intensity 515 nm was used

386 for the plots. The error bars represent the standard deviation of three different measurements.

387

388 **Fig.4.** (A) Aptamer release from the GO surface by the addition of (natural tropomyosin from

389 black tiger prawn) TM: Increase in the fluorescence intensity with increase in the

390 concentration of protein : a: 0, b: 0.01, c: 0.1, d: 0.2, e: 0.5, f: 1, g: 2, h: 5, i: 10, j: 20, k: 50

391 $\mu\text{g/ml}$. (B) The calibration plot fluorescence intensity against TM concentration ($\mu\text{g/ml}$) the

392 of TMT2 at 515 nm. The fluorescence spectra were recorded by exciting at 470 ± 10 nm and

393 the emission intensity 515 nm was used for the plots. The error bars represent the standard
394 deviation of three different measurements.

395

396 **Fig.5.** The cross-reactivity response of GO- TMT2 aptamer (15 $\mu\text{g/ml}$ -25 nM) fluorescence
397 assay for different tropomyosin protein samples and irrelevant samples with the
398 concentrations of 5 $\mu\text{g/ml}$. TM Proteins: Black Tiger Prawn Tropomyosin (BTP TM), Oyster
399 TM, Anisakis TM, Prawn TM and irrelevant protein: BSA and Streptavidin. The fluorescence
400 intensity of each sample obtained by exciting at 470 ± 10 nm and the emission intensity 515
401 nm was used for the plots. The error bars represent the standard deviation of three different
402 measurements.

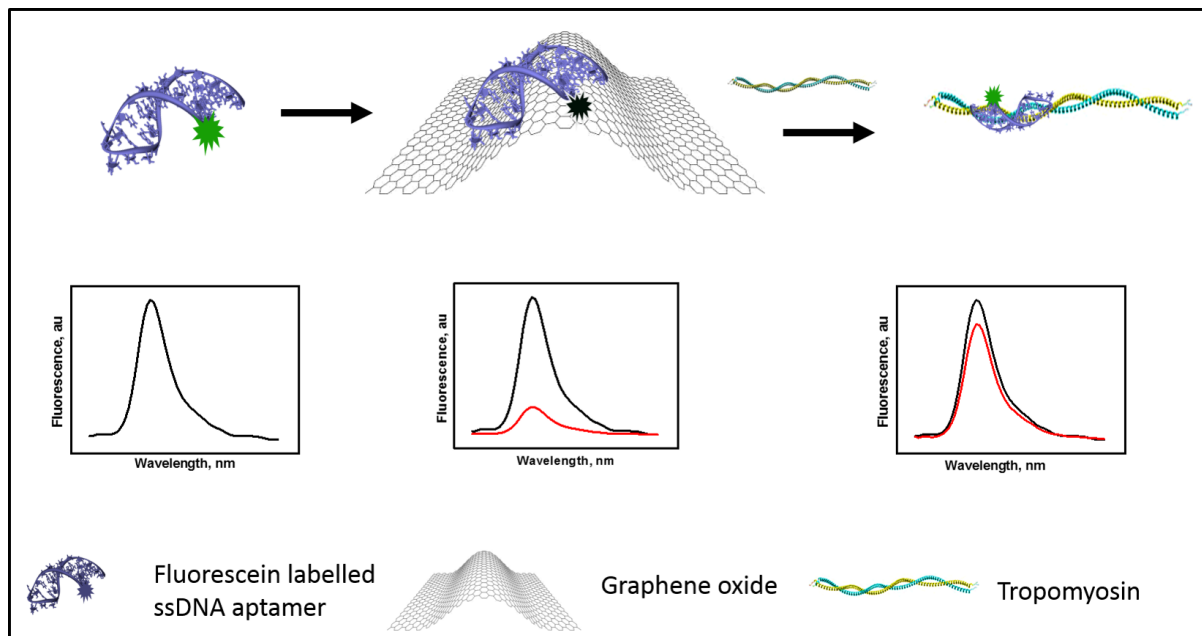
403

404

405

406
407
408
409

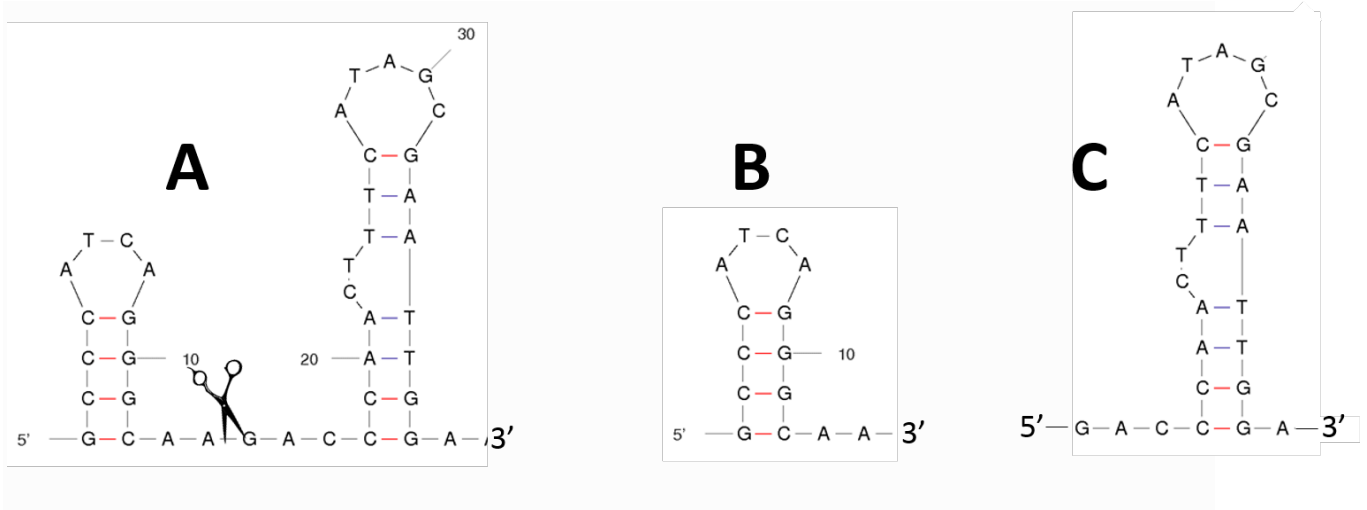
Scheme 1.



410
411
412
413
414
415
416
417
418
419
420
421
422
423
424
425
426
427
428
429
430
431
432
433
434
435

436
437
438
439

Fig. 1



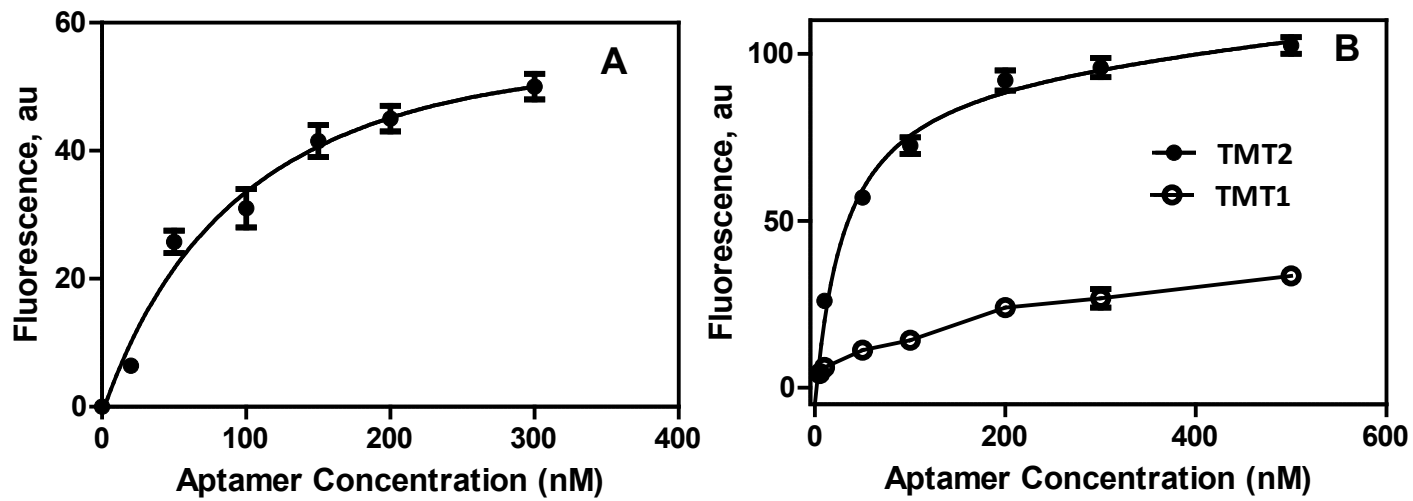
440

441
442
443
444
445
446
447

448

449

Fig. 2



450

451

452

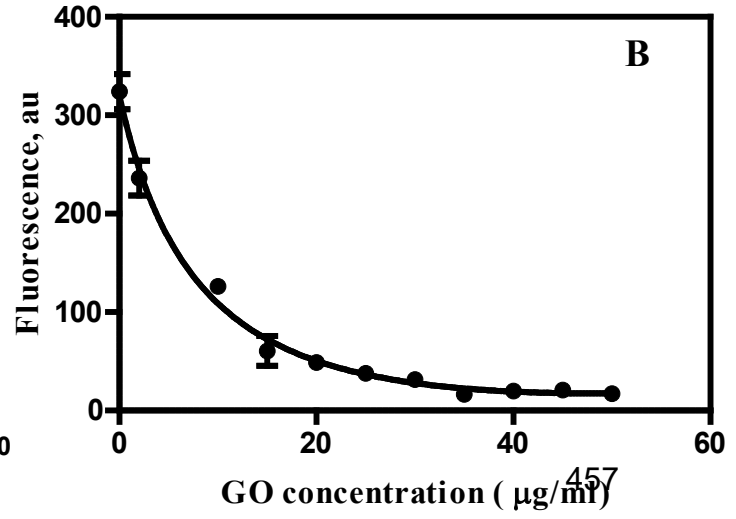
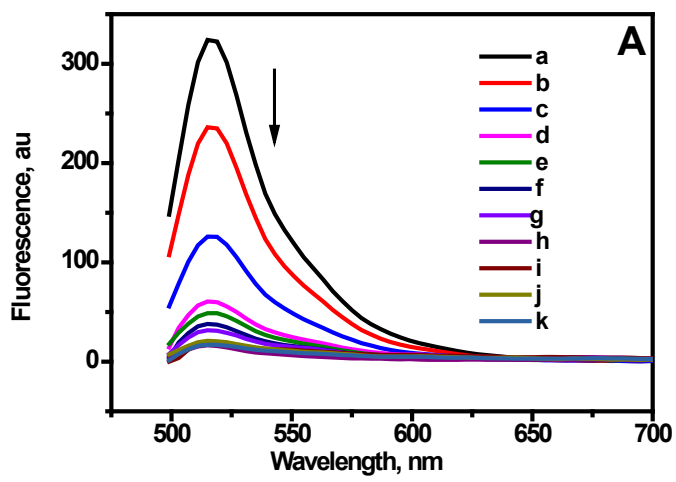
453

454

455

Fig. 3

456



458

459

460

461

462

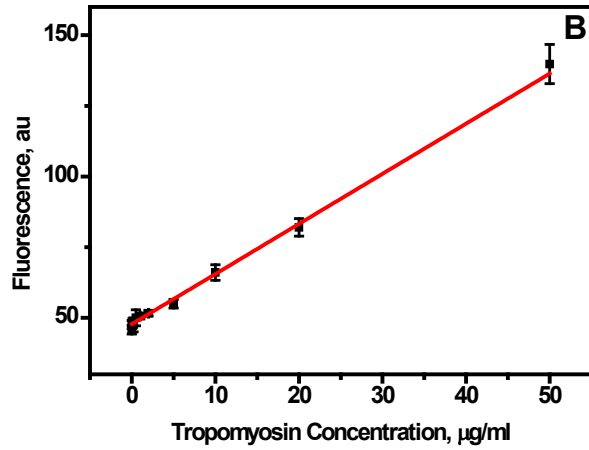
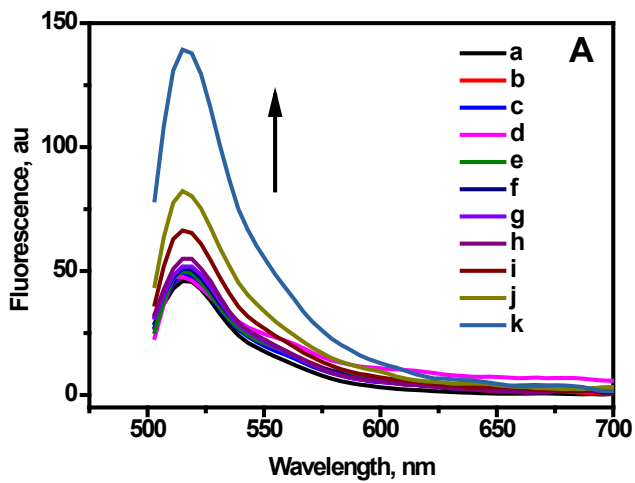
463

464

465

466

Fig. 4



467

468

469

470

471

472

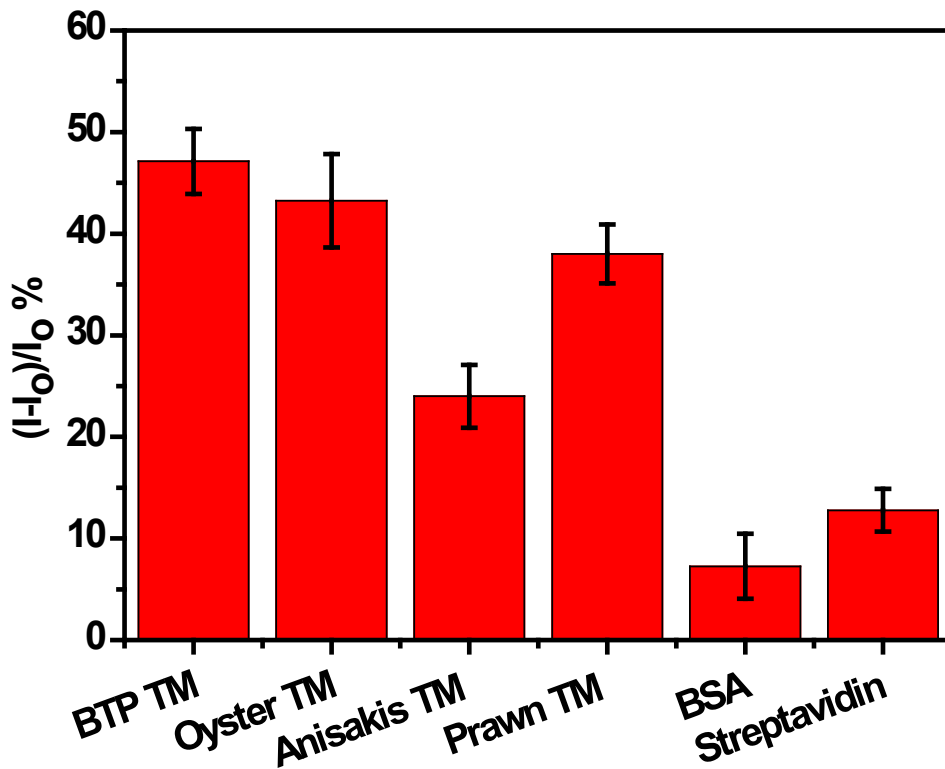
473

474

475

476

477 Fig. 5



478

479

480

481

482

483

484

5. References

- 485 Abdel Rahman, A. M., Kamath, S. D., Gagné, S. b., Lopata, A. L., & Helleur, R. (2013).
486 Comprehensive proteomics approach in characterizing and quantifying allergenic
487 proteins from northern shrimp: toward better occupational asthma prevention. *Journal*
488 *of proteome research*, 12(2), 647-656.
- 489 Alhadrami, H., Chinnappan, R., Eissa, S., Rahamn, A. A., & Zourob, M. (2017). High
490 affinity truncated DNA aptamers for the development of fluorescence based
491 progesterone biosensors. *Anal Biochem*.
- 492 Alhadrami, H. A., Chinnappan, R., Eissa, S., Rahamn, A. A., & Zourob, M. (2017). High
493 affinity truncated DNA aptamers for the development of fluorescence based
494 progesterone biosensors. *Analytical Biochemistry*, 525, 78-84.
- 495 Amouzadeh Tabrizi, M., Shamsipur, M., Saber, R., Sarkar, S., & Ebrahimi, V. (2017). A high
496 sensitive visible light-driven photoelectrochemical aptasensor for shrimp allergen
497 tropomyosin detection using graphitic carbon nitride-TiO₂ nanocomposite.
498 *Biosensors and Bioelectronics*, 98(Supplement C), 113-118.
- 499 Asnoussi, A., Aibinu, I. E., Gasser, R. B., Lopata, A. L., & Smooker, P. M. (2017).
500 Molecular and immunological characterisation of tropomyosin from *Anisakis*
501 *pegreffii*. *Parasitol Res*, 116(12), 3291-3301.
- 502 Chinnappan, R., AlAmer, S., Eissa, S., Rahamn, A. A., Salah, K. M. A., & Zourob, M.
503 (2018). Fluorometric graphene oxide-based detection of *Salmonella enteritis* using a
504 truncated DNA aptamer. *Microchimica Acta*, 185(1), 61.
- 505 Cowperthwaite, M. C., & Ellington, A. D. (2008). Bioinformatic analysis of the contribution
506 of primer sequences to aptamer structures. *Journal of molecular evolution*, 67(1), 95-
507 102.
- 508 Ding, S., Cargill, A. A., Das, S. R., Medintz, I. L., & Claussen, J. C. (2015). Biosensing with
509 förster resonance energy transfer coupling between fluorophores and nanocarbon
510 allotropes. *Sensors*, 15(6), 14766-14787.
- 511 Fernandes, T. J. R., Costa, J., Oliveira, M. B. P. P., & Mafra, I. (2015). An overview on fish
512 and shellfish allergens and current methods of detection. *Food and Agricultural*
513 *Immunology*, 26(6), 848-869.
- 514 Fuller, H. R., Goodwin, P. R., & Morris, G. E. (2006). An enzyme-linked immunosorbent
515 assay (ELISA) for the major crustacean allergen, tropomyosin, in food. *Food and*
516 *agricultural immunology*, 17(1), 43-52.
- 517 Gao, L., Li, Q., Li, R., Yan, L., Zhou, Y., Chen, K., & Shi, H. (2015). Highly sensitive
518 detection for proteins using graphene oxide-aptamer based sensors. *Nanoscale*, 7(25),
519 10903-10907.
- 520 Hasegawa, H., Savory, N., Abe, K., & Ikebukuro, K. (2016). Methods for improving aptamer
521 binding affinity. *Molecules*, 21(4), 421.
- 522 Jayasena, S. D. (1999). Aptamers: an emerging class of molecules that rival antibodies in
523 diagnostics. *Clinical chemistry*, 45(9), 1628-1650.
- 524 Kamath, S. D., Abdel Rahman, A. M., Komoda, T., & Lopata, A. L. (2013). Impact of heat
525 processing on the detection of the major shellfish allergen tropomyosin in crustaceans
526 and molluscs using specific monoclonal antibodies. *Food Chem*, 141(4), 4031-4039.
- 527 Kamath, S. D., Thomassen, M. R., Saptarshi, S. R., Nguyen, H. M., Aasmoe, L., Bang, B. E.,
528 & Lopata, A. L. (2014). Molecular and immunological approaches in quantifying the
529 air-borne food allergen tropomyosin in crab processing facilities. *Int J Hyg Environ*
530 *Health*, 217(7), 740-750.

- 531 Kaur, H., & Yung, L. Y. (2012). Probing high affinity sequences of DNA aptamer against
532 VEGF165. *PLoS One*, 7(2), e31196.
- 533 Khanaruksombat, S., Srisomsap, C., Chokchaichamnankit, D., Punyarit, P., & Phiriyangkul,
534 P. (2014). Identification of a novel allergen from muscle and various organs in banana
535 shrimp (*Fenneropenaeus merguensis*). *Annals of Allergy, Asthma & Immunology*,
536 113(3), 301-306.
- 537 Kim, M.-J., Kim, H.-I., Kim, J.-H., Suh, S.-M., & Kim, H.-Y. (2019). Rapid on-site detection
538 of shrimp allergen tropomyosin using a novel ultrafast PCR system. *Food Science and
539 Biotechnology*, 28(2), 591-597.
- 540 Koeberl, M., Clarke, D., & Lopata, A. L. (2014). Next generation of food allergen
541 quantification using mass spectrometric systems. *Journal of proteome research*,
542 13(8), 3499-3509.
- 543 Koeberl, M., Kamath, S. D., Saptarshi, S. R., Smout, M. J., Rolland, J. M., O'Hehir, R. E., &
544 Lopata, A. L. (2014). Auto-induction for high yield expression of recombinant novel
545 isoallergen tropomyosin from King prawn (*Melicertus latisulcatus*) for improved
546 diagnostics and immunotherapeutics. *Journal of immunological methods*, 415, 6-16.
- 547 Kwon, Y. S., Raston, N. H. A., & Gu, M. B. (2014). An ultra-sensitive colorimetric detection
548 of tetracyclines using the shortest aptamer with highly enhanced affinity. *Chemical
549 Communications*, 50(1), 40-42.
- 550 Lapa, S. A., Chudinov, A. V., & Timofeev, E. N. (2016). The Toolbox for Modified
551 Aptamers. *Mol Biotechnol*, 58(2), 79-92.
- 552 Le, T. T., Chumphukam, O., & Cass, A. E. G. (2014). Determination of minimal sequence for
553 binding of an aptamer. A comparison of truncation and hybridization inhibition
554 methods. *RSC Advances*, 4(88), 47227-47233.
- 555 Lopata, A. L., Kleine-Tebbe, J., & Kamath, S. D. (2016). Allergens and molecular
556 diagnostics of shellfish allergy: Part 22 of the Series Molecular Allergology. *Allergo
557 journal international*, 25(7), 210-218.
- 558 Lupinek, C., Wollmann, E., Baar, A., Banerjee, S., Breiteneder, H., Broecker, B. M., Bublin,
559 M., Curin, M., Flicker, S., Garmatiuk, T., Hochwallner, H., Mittermann, I., Pahr, S.,
560 Resch, Y., Roux, K. H., Srinivasan, B., Stentzel, S., Vrtala, S., Willison, L. N.,
561 Wickman, M., Lødrup-Carlson, K. C., Antó, J. M., Bousquet, J., Bachert, C., Ebner,
562 D., Schleiderer, T., Harwanegg, C., & Valenta, R. (2014). Advances in allergen-
563 microarray technology for diagnosis and monitoring of allergy: the MeDALL
564 allergen-chip. *Methods (San Diego, Calif.)*, 66(1), 106-119.
- 565 Nugraha, R., Kamath, S. D., Johnston, E., Zenger, K. R., Rolland, J. M., O'Hehir, R. E., &
566 Lopata, A. L. (2018). Rapid and comprehensive discovery of unreported shellfish
567 allergens using large-scale transcriptomic and proteomic resources. *J Allergy Clin
568 Immunol*, 141(4), 1501-1504.e1508.
- 569 Rahman, A. M. A., Gagné, S., & Helleur, R. J. (2012). Simultaneous determination of two
570 major snow crab aeroallergens in processing plants by use of isotopic dilution tandem
571 mass spectrometry. *Analytical and bioanalytical chemistry*, 403(3), 821-831.
- 572 Rahman, A. M. A., Kamath, S., Lopata, A. L., & Helleur, R. J. (2010). Analysis of the
573 allergenic proteins in black tiger prawn (*Penaeus monodon*) and characterization of
574 the major allergen tropomyosin using mass spectrometry. *Rapid communications in
575 mass spectrometry*, 24(16), 2462-2470.
- 576 Rahman, A. M. A., Kamath, S. D., Lopata, A. L., Robinson, J. J., & Helleur, R. J. (2011).
577 Biomolecular characterization of allergenic proteins in snow crab (*Chionoecetes
578 opilio*) and de novo sequencing of the second allergen arginine kinase using tandem
579 mass spectrometry. *Journal of proteomics*, 74(2), 231-241.

- 580 Rahman, A. M. A., Lopata, A. L., Randell, E. W., & Helleur, R. J. (2010). Absolute
581 quantification method and validation of airborne snow crab allergen tropomyosin
582 using tandem mass spectrometry. *Analytica chimica acta*, 681(1-2), 49-55.
- 583 Ruethers, T., Taki, A. C., Johnston, E. B., Nugraha, R., Le, T. T. K., Kalic, T., McLean, T.
584 R., Kamath, S. D., & Lopata, A. L. (2018). Seafood allergy: A comprehensive review
585 of fish and shellfish allergens. *Mol Immunol*, 100, 28-57.
- 586 Seiki, K., Oda, H., Yoshioka, H., Sakai, S., Urisu, A., Akiyama, H., & Ohno, Y. (2007). A
587 reliable and sensitive immunoassay for the determination of crustacean protein in
588 processed foods. *Journal of agricultural and food chemistry*, 55(23), 9345-9350.
- 589 Sharma, G. M., Khuda, S. E., Parker, C. H., Eischeid, A. C., & Pereira, M. (2016). Detection
590 of Allergen Markers in Food: Analytical Methods. *Food Safety: Innovative Analytical*
591 *Tools for Safety Assessment*, 65-121.
- 592 Shen, H.-W., Cao, M.-J., Cai, Q.-F., Ruan, M.-M., Mao, H.-Y., Su, W.-J., & Liu, G.-M.
593 (2012). Purification, cloning, and immunological characterization of arginine kinase,
594 a novel allergen of Octopus fangsiao. *Journal of agricultural and food chemistry*,
595 60(9), 2190-2199.
- 596 Stobiecka, M., Dworakowska, B., Jakiela, S., Lukasiak, A., Chalupa, A., & Zembrzycki, K.
597 (2016). Sensing of survivin mRNA in malignant astrocytes using graphene oxide
598 nanocarrier-supported oligonucleotide molecular beacons. *Sensors and Actuators B:*
599 *Chemical*, 235, 136-145.
- 600 Werner, M. T., Fæste, C. K., & Egaas, E. (2007). Quantitative sandwich ELISA for the
601 determination of tropomyosin from crustaceans in foods. *Journal of agricultural and*
602 *food chemistry*, 55(20), 8025-8032.
- 603 Yang, Y., Asiri, A. M., Tang, Z., Du, D., & Lin, Y. (2013). Graphene based materials for
604 biomedical applications. *Materials today*, 16(10), 365-373.
- 605 Zhang, H., Lu, Y., Ushio, H., & Shiomi, K. (2014). Development of sandwich ELISA for
606 detection and quantification of invertebrate major allergen tropomyosin by a
607 monoclonal antibody. *Food Chemistry*, 150, 151-157.
- 608 Zhang, H., Zhang, H., Aldalbahi, A., Zuo, X., Fan, C., & Mi, X. (2017). Fluorescent
609 biosensors enabled by graphene and graphene oxide. *Biosensors and Bioelectronics*,
610 89, 96-106.
- 611 Zhang, Y., Wu, Q., Wei, X., Zhang, J., & Mo, S. (2017). DNA aptamer for use in a
612 fluorescent assay for the shrimp allergen tropomyosin. *Microchimica Acta*, 184(2),
613 633-639.
- 614 Zhou, J., Battig, M. R., & Wang, Y. (2010). Aptamer-based molecular recognition for
615 biosensor development. *Analytical and Bioanalytical Chemistry*, 398(6), 2471-2480.

616